J|A|C|S
ARTICLES
Published on Web 12/24/2002

Induction of a Remarkable Conformational Change in a Human Telomeric Sequence by the Binding of Naphthyridine Dimer: Inhibition of the Elongation of a Telomeric Repeat by Telomerase

Kazuhiko Nakatani,*[,†,‡] Shinya Hagihara,[†] Shinsuke Sando,[†] Shigeru Sakamoto,[§] Kentaro Yamaguchi,[§] Chihaya Maesawa,[||] and Isao Saito*[,†]

Contribution from the Department of Synthetic Chemistry and Biological Chemistry, Faculty of Engineering, Kyoto University, Kyoto 606-8501, Japan, PRESTO, Japan Science and Technology Corporation (JST), Kawaguchi City, Saitama 332-0012, Japan, Chemical Analysis Center, Chiba University, Chiba 263-8522, Japan, and Department of Pathology, Iwate Medical University School of Medicine, Uchimaru 19-1, 020-8505 Morioka, Japan

Received May 27, 2002; E-mail: nakatani@sbchem.kyoto-u.ac.jp; saito@sbchem.kyoto-u.ac.jp

Abstract: The binding of a dimeric form of the 2-amino-1,8-naphthyridine derivative (naphthyridine dimer) to a human telomeric sequence, TTAGGG, was investigated by UV melting, CD spectra, and CSI-MS measurements. Both the 9-mer d(TTAGGGTTA) and the 15-mer d(TTAGGGTTAGGGTTA) showed apparent melting temperatures (T_m) of 45.6 and 63.6 °C, respectively, in the presence of naphthyridine dimer (30 μM) in sodium cacodylate buffer (50 mM, pH 7.0) containing 100 mM NaCl. The CD spectra at 235 and 255 nm of the 9-mer increased in intensity accompanied with strong induced CDs at 285 and 340 nm upon complex formation with naphthyridine dimer. UV titration of the binding of naphthyridine dimer to the 9-mer at 320 nm showed a hypochromism of the spectra. A Scatchard plot of the data showed the presence of multiple binding sites with different association constants. Cold spray ionization mass spectrometry of the complex between naphthyridine dimer and the 9-mer clearly showed that one to three molecules of the ligand bound to the dimer duplex of the 9-mer. Telomeric repeat elongation assay showed that the binding of naphthyridine dimer to the telomeric sequence inhibits the elongation of the sequence by telomerase.

Introduction

The ends of human chromosomes, the telomeres, consist of duplex DNA and 3′ single-stranded overhangs of G-rich TTAGGG sequences. The single-stranded region of the telomere forms a variety of higher-order structures, including the G-quadruplex.[1−4] Because telomeric length is maintained by the enzyme telomerase in most tumor cell lines but not in normal healthy cells, drugs that stabilize the G-quadruplex and hence interfere with the elongation of the telomere by telomerase are potential anticancer agents.[5−8] DNA intercalators with wider planar structures than those that target the B-form DNA duplex selectively bind to and stabilize the G-quadruplex.[5,9−16] We have reported previously that a dimeric form of the 2-amino-1,8-naphthyridine derivative **1** (naphthyridine dimer) strongly binds to a G-G mismatch in duplex DNA.[17−19] NMR analysis of the complex formed between **1** and the G-G-mismatch-containing duplex d(CATCGGATG)$_2$ verified the zigzag intercalation of two naphthyridine rings (Figure 1a).[20] Each naphthyridine group formed hydrogen bonds to one of the mismatched guanines,

[†] Kyoto University.
[‡] JST.
[§] Chiba University.
[||] Iwate Medical University School of Medicine.

(1) Sen, D.; Gilbert, W. *Nature* **1988**, *334*, 364−366.
(2) Oka, Y.; Thomas, C. A., Jr. *Nucleic Acids Res.* **1987**, *15*, 8877−8898.
(3) Sundquist, W. I.; Klug, A. *Nature* **1989**, *342*, 825−829.
(4) Griffith, J. D.; Comeau, L.; Rosenfield, S.; Stansel, R. M.; Bianchi, A.; Moss, H.; de Lange, T. *Cell* **97**, 503−514.
(5) Shi, D.-F.; Wheelhouse, R. T.; Sun, D.; Hurley, L. H. *J. Med. Chem.* **2001**, *44*, 4509−4523.
(6) Kerwin, S. M. *Curr. Pharm. Des.* **2000**, *6*, 441−471.
(7) Jenkins, T. C. *Curr. Med. Chem.* **2000**, *7*, 99−115.
(8) Mergny, J.-L.; Hélène, C. *Nat. Med.* **1998**, *4*, 1366−1367.
(9) Perry, P. J.; Jenkins, T. C. *Exp. Opin. Invest. Drugs* **1999**, *8*, 1981−2008.
(10) Han, H.; Langley, D. R.; Rangan, A.; Hurley, L. H. *J. Am. Chem. Soc.* **2001**, *123*, 8902−8913.
(11) Mergny, J.-L.; Lacroix, L.; Teulade-Fichou, M. P.; Hounsou, C.; Guittat, L.; Hoarau, M.; Arimondo, P. B.; Vigneron, J. P.; Lehn, J. M.; Riou, J.-F.; Garestier, T.; Hélène, C. *Proc. Natl. Acad. Sci. U.S.A.* **2001**, *98*, 3062−3067.
(12) Kim, M.-Y.; Vankayalapati, H.; Shin-ya, K.; Wierzba, K.; Hurley, L. H. *J. Am. Chem. Soc.* **2002**, *124*, 2098−2099.
(13) Koppel, F.; Riou, J.-F.; Laoui, A.; Malliet, P.; Arimondo, P. B.; Labit, D.; Petigenet, O.; Hélène, C.; Mergny, J.-L. *Nucleic Acids Res.* **2001**, *29*, 1087−1096.
(14) Rangan, A.; Fedoroff, O. Yu.; Hurley, L. H. *J. Biol. Chem.* **2001**, *276*, 4640−4646.
(15) Harrison, R. J.; Gowan, S. M.; Kelland, L. R.; Neidle, S. *Bioorg. Med. Chem. Lett.* **1999**, *9*, 2463−2468.
(16) Read, M.; Harrison, R. J.; Romagnoli, B.; Tanious, F. A.; Gowan, S. H.; Reszka, A. P.; Wilson, W. D.; Kelland, L. R.; Neidle, S. *Proc. Natl. Acad. Sci. U.S.A.* **2001**, *98*, 4844.
(17) Nakatani, K.; Sando, S.; Saito, I. *Nat. Biotechnol.* **2001**, *19*, 51−55.
(18) Nakatani, K.; Sando, S.; Saito, I. *Bioorg. Med. Chem.* **2001**, *9*, 2381−2385.
(19) Smith, E. A.; Kyo, M.; Kumasawa, H.; Nakatani, K.; Saito, I.; Corn, R. M. *J. Am. Chem. Soc.* **2002**, *124*, 6810−6811.
(20) Nakatani, K.; Sando, S.; Kumasawa, H.; Kikuchi, J.; Saito, I. *J. Am. Chem. Soc.* **2001**, *123*, 12650−12657.

10.1021/ja027055g CCC: $25.00

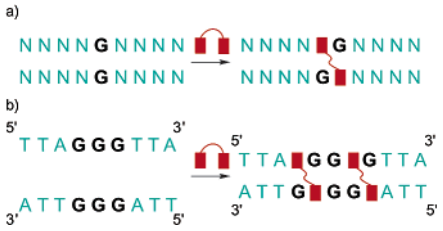

Figure 1. Illustrations of (a) a zigzag intercalation of **1** into a duplex containing a single G-G mismatch and (b) a proposed binding of **1** to a pair of a single-stranded overhang of a human telomeric sequence.

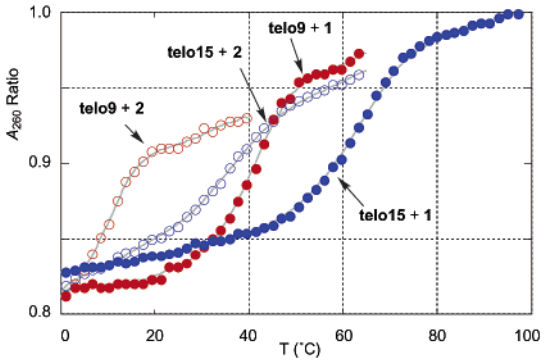

Figure 2. Thermal-denaturation profiles of **telo9** (red) and **telo15** (blue) in the presence of **1** (filled circle) and **2** (open circle) (30 μM). Absorbance at 260 nm (A_{260}) of the oligomer (5 μM, strand concentration) in sodium cacodylate buffer (pH 7.0) and NaCl (100 mM) was measured from 0 to 100 °C with a heating rate of 1 °C/min. The A_{260} ratio, defined as A_{260} (T)/A_{260} (100 °C), was plotted against temperature T (°C). Only parts of the plots are shown for clarity.

and the resulting naphthyridine−guanine pairs stacked with each other within a duplex π-stack. Because of the guanine-rich nature of the telomeric sequence, we predicted that **1** should act as a molecular glue in the assembly of two telomeric sequences by binding strongly to G-G mismatches in the hypothetical duplex of a telomeric dimer (Figure 1b). We here report that **1** binds strongly to the single-stranded overhang of a human telomeric sequence, regardless of the initial secondary structure of the sequence. Telomeric repeat elongation assay showed that **1** binding to the telomeric repeat inhibits the elongation of the sequence by the telomerase.

Results and Discussion

Thermal Denaturation Study of the Telomeric Sequence in the Presence of 1. The binding of **1** to a human telomeric sequence was studied by measuring the thermal-denaturation profile in the absence and presence of the drug. We monitored a change of the absorption at 260 nm, which is a typical index for the conformational change from single- to double-stranded DNA (Figure 2). Both the 9-mer d(TTAGGGTTA) (**telo9**) and the 15-mer d(TTAGGGTTAGGGTTA) (**telo15**) showed a linear increase in UV absorption at 260 nm upon heating in sodium cacodylate buffer (50 mM, pH 7.0) containing 100 mM NaCl. In marked contrast, sigmoidal denaturation curves indicative of a transition between two secondary structures were produced for both oligomers in the presence of **1** (30 μM). The apparent melting temperatures (T_m) of the secondary structures of **telo9** and **telo15** in the presence of **1** were 45.6 and 63.6 °C, respectively. Because the amide bond in **1** is gradually hydrolyzed at a high temperature in an aqueous solution, we did not start T_m measurements from the high temperature. Therefore, the reported melting temperatures may be overestimated to some extent from

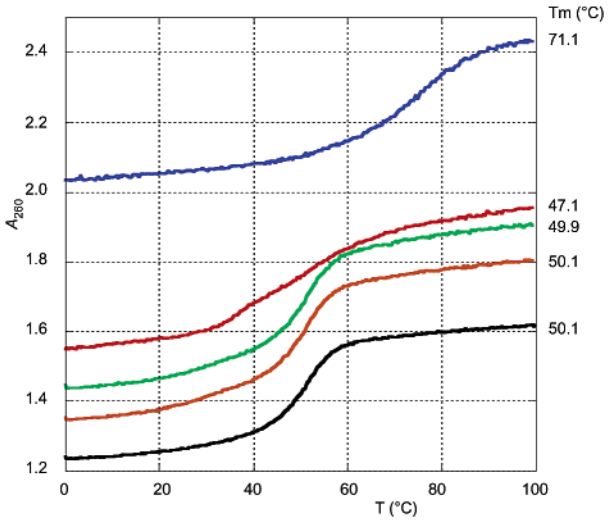

Figure 3. Thermal denaturation profiles of the duplex **telo15**/**telo15-c** in the absence and presence of **1**, **2**, **3**, and **TMPyP4** (30 μM). Absorbance at 260 nm (A_{260}) of the oligomer (5 μM) was plotted against temperature T (°C). Key: duplex (black), duplex + **1** (red), duplex + **2** (green), duplex + **3** (orange), and duplex + **TMPyP4** (blue). The apparent melting temperatures are shown on the right.

the real T_m values. A small structural change from **1** to the 2-aminoquinoline−naphthyridine hybrid **2**[20] resulted in a dramatic decrease in the apparent T_m of **telo9** and **telo15** to 13.1 and 33.7 °C, respectively. The monomeric 2-aminonaphthyridine derivative **3**[21] induced only a weak change in the UV absorbance of **telo15**, producing an apparent T_m of 19.2 °C (Figure S1 in the Supporting Information). We have previously shown that the binding of **2** to a G-G mismatch is much weaker than the binding of **1**.[20] The T_m of the duplex formed between **telo15** and its complement d(TAACCCTAACCCTAA) (**telo15-c**) did not increase at all in the presence of **1**, indicating that **1** binds specifically to the single-stranded overhang of a telomeric repeat (Figure 3). 5,10,15,20-Tetra(*N*-methyl-4-pyridyl)porphine (**TMPyP4**),[5,10,22,23] which binds to the G-quadruplex, strongly increased the T_m of the **telo15/telo15-c** duplex, but did not produce

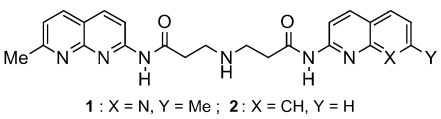

1 : X = N, Y = Me ; **2** : X = CH, Y = H

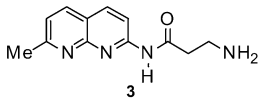

3

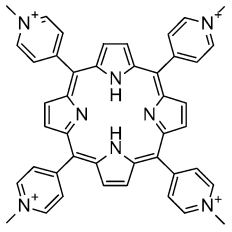

TMPyP4

(21) Nakatani, K.; Sando, S.; Saito, I. *J. Am. Chem. Soc.* **2000**, *122*, 2172−2177.
(22) Wheelhouse, R. T.; Sun, D.; Han, H.; Han, F. X.; Hurley, L. H. *J. Am. Chem. Soc.* **1998**, *120*, 3261−3262.
(23) Han, F. X.; Wheelhouse, R. T.; Hurley, L. H. *J. Am. Chem. Soc.* **1999**, *121*, 3561−3570.

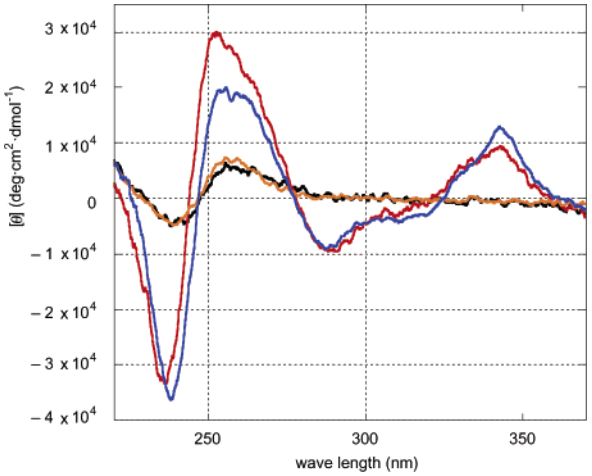

Figure 4. CD spectra of **telo9** and **telo15** in the absence and presence of **1** (30 μM). CD measurements were carried out with 5 μM DNA in 100 mM NaCl and 10 mM sodium cacodylate buffer (pH 7.0) at 25 °C. Key: **telo9** (black), **telo9** + **1** (red), **telo15** (orange), **telo15** + **1** (blue).

a sigmoidal denaturation curve regarding an absorption change at 260 nm when binding to **telo15** (Figure S2 in the Supporting Information). This suggests that **1** and **TMPyP4** use different mechanisms to stabilize telomeric sequences.

Circular Dichroism Spectra of the Complex of the Telomeric Sequence and 1. Significant circular dichroism (CD) spectral changes were observed in **telo9** and **telo15** in the presence of **1** (Figure 4). In sodium cacodylate buffer (10 mM, pH 7.0) containing NaCl (100 mM) at 25 °C, the CD spectra of both **telo9** and **telo15** were uncharacteristic, indicating that the structures of both oligomers are random coils under these conditions. Upon the addition of **1** (30 μM), the CD spectra at 235 and 255 nm increased in intensity accompanied with strong induced CDs at 285 and 340 nm, indicating that these oligomers formed distinct secondary structures upon binding with **1**. The remarkable CD changes in **telo9** were specifically induced with **1** at 25 °C. Neither **2** nor **3** had such effects on the CD spectra at this temperature. These observations are fully consistent with the results of thermal denaturation studies, because the melting temperatures of the secondary structure of **telo9** induced by the binding of **2** and **3** were much lower than 25 °C. Similar CD profiles were observed for **telo15** in the absence and presence of **1**.

Short oligomers of a telomeric sequence tend to form a parallel G-quadruplex in the presence of the potassium cation.[24] The parallel G-quadruplex shows strong positive CD values at 270 nm and negative CD values at 240 nm.[25] In the presence of 50 mM KCl, the CD spectrum for **telo15** changed its positive maximum to 265 nm from 255 nm in 100 mM NaCl (Figure 5). The weak but distinct spectral change of **telo15** depending on the presence of potassium cation indicated a transition of the secondary structure from a random coil to a parallel G-quadruplex. Under the conditions containing 50 mM KCl, the CD spectral change in **telo15** induced by **1** is not as large as those observed in 100 mM NaCl. The stabilization of the G-quadruplex by potassium cation resulted in a lowering of the molar fraction of the secondary structure induced by **1** binding, suggesting that the **telo15**−**1** complex is in equilibrium with the parallel G-quadruplex under the conditions.

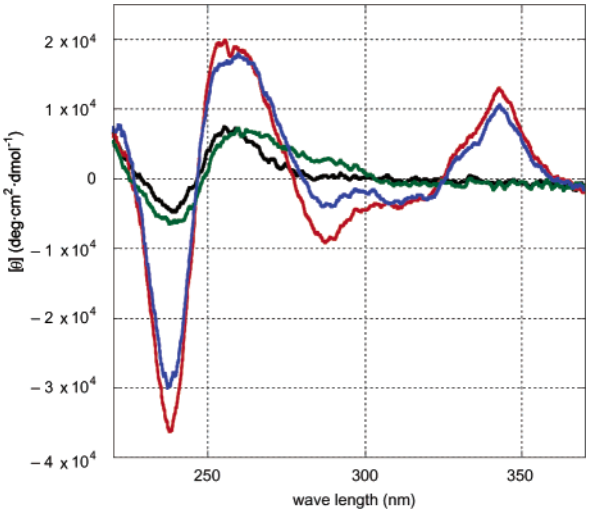

Figure 5. CD spectrum of **telo15** in the presence and absence of **1** (30 μM). The CD spectrum of **telo15** (d(TTA GGG TTA GGG TTA)-3′) (5 μM, strand concentration) was measured at 25 °C in a sodium cacodylate buffer (10 mM, pH 7.0) containing NaCl (100 mM) or KCl (50 mM). Key: **telo15** in NaCl (black), KCl (green), NaCl + **1** (red), and KCl + **1** (blue).

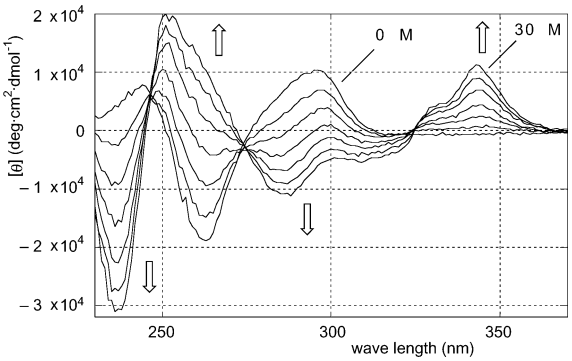

Figure 6. CD spectral change of the antiparallel G-quadruplex of **telo22** d(AGGGTTAGGGTTAGGGTTAGGG) upon addition of **1**. CD measurements were carried out with 5 μM DNA in 100 mM NaCl and 10 mM sodium phosphate buffer (pH 7.0) at 7 °C. The concentration of **1** was 0, 5, 10, 15, 20, 25, and 30 μM.

The DNA 22-mer d(AGGGTTAGGGTTAGGGTTAGGG) (**telo22**), consisting of four tandem repeats of a human telomeric sequence, forms an antiparallel G-quadruplex[26] that shows typical CD spectra with positive and negative CDs at 290 and 265 nm, respectively.[25] Upon the addition of **1** to an antiparallel G-quadruplex, dramatic changes in the CD spectra were induced (Figure 6). The CD spectrum of **telo22** in the presence of 30 μM **1** was indistinguishable from that of **telo15** measured in the presence of **1**. These results suggest that **1** binds to a human telomeric sequence regardless of the initial secondary structure or length of the sequence, and produces a unique structure.

UV Titration for the Binding of 1 to the Telomeric Sequence. The binding of **1** to a telomeric sequence was further analyzed by UV titration to gain some insights into the **1** binding. UV titration was performed by adding **telo9** (0−17.5 μM) to **1** while keeping the **1** concentration constant (20 μM) at 20 °C (Figure 7). In the absence of **telo9**, characteristic UV absorptions of **1** were observed at 320 and 335 nm. By increasing the concentration of **telo9**, the intensity of the unique absorption decreased, whereas the absorption over 340 nm increased. These spectral changes suggested the intercalative binding of **1** upon

(24) Wang, Y.; Patel, D. J. *Biochemistry* **1992**, *31*, 8112−8119.
(25) Williamson, J. R. *Curr. Opin. Struct. Biol.* **1993**, *3*, 357−362.
(26) Wang, Y.; Patel, D. J *Structure* **1993**, *1*, 263−282.

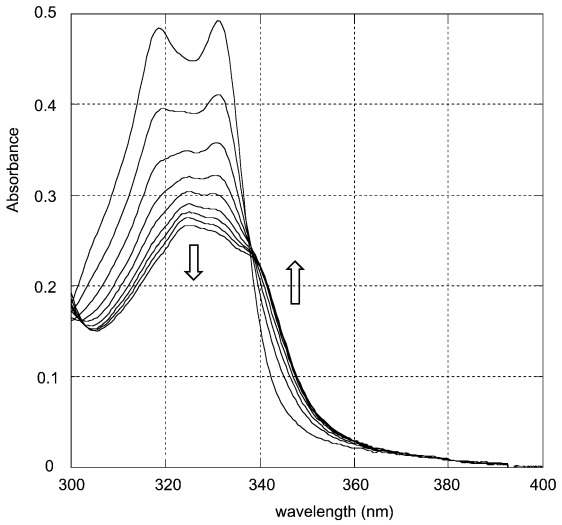

Figure 7. UV absorption spectra of **1** (20 μM) in the presence of various concentrations of **telo9**. The experiments were conducted in a sodium cacodylate buffer (10 mM, pH 7.0) containing NaCl (100 mM) at 20 °C. The concentration of **telo9** was 0, 1.25, 2.5, 5, 7.5, 10, 12.5, 15, and 17.5 μM from the top to bottom.

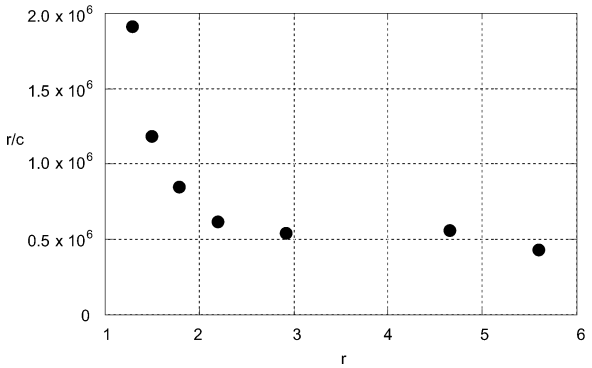

Figure 8. A Scatchard plot of the data at 320 nm shown in Figure 7.

complex formation with **telo9**. A Scatchard plot of the data points obtained at 320 nm showed a concave-up curve with an *x*-asymptote (Figure 8). This type of curve in a Scatchard plot suggests the presence of nonspecific binding in addition to the multiple classes of binding sites with differing K_D values and cooperativity for the binding. Due to the cooperativity and the expected allosterism from the large conformational change of **telo9** by **1** binding, the precise stoichiometry for the binding and, thus, the binding constants could not be determined from the plots. The continuous variation method (Job's plot) is often used for determining the stoichiometry of the binding. However, it is not applicable for the analysis of the binding of **1** to **telo9**, because the method assumes that all the sites for the ligand binding are equivalent and independent.[27] The number of molecules of **1** bound to **telo9** at saturation was very roughly estimated to be between three and four because the curve almost reaches a plateau over the range of *r* exceeding 3.

Cold Spray Ionization Mass Spectrometry for the Complex of 1 and the Telomeric Sequence. DNA−drug complexes could be directly determined by electrospray ionization mass spectrometry (ESI-MS).[28] We have analyzed a complex produced from **telo9** and **1** by an innovative technique of cold spray ionization (CSI) developed by Yamaguchi, which is suitable for the ionization of the noncovalent complexes (Figure 9).[29−33] CSI-MS of **telo9** (18 μM in 40% v/v methanol containing 100 mM ammonium acetate) showed two ions (m/z = 921.6 and 1383.3) corresponding to $[\mathbf{telo9}]^{3-}$ and $[\mathbf{telo9}]^{2-}$. In the presence of **1** (85 μM), three distinct ions, $\{2[\mathbf{telo9}] + [\mathbf{1}]\}^{4-}$ (m/z = 1494.4), $\{2[\mathbf{telo9}] + 2[\mathbf{1}]\}^{4-}$ (m/z = 1604.7), and $\{2[\mathbf{telo9}] + 3[\mathbf{1}]\}^{4-}$ (m/z = 1717.9), were detected. These results showed that **telo9** forms a dimer duplex by the binding of one to three molecules of **1** under these conditions and are consistent with the results obtained by the UV titration experiments.

Inhibitory Effects of 1 Binding on the Telomeric Repeat Elongation. The ligands stabilizing the G-quadruplex exhibit inhibitory effects on the telomeric elongation by telomerase in a concentration-dependent manner. As discussed above, **1** binds to a telomeric repeat and forms unique structures that are different from the G-quadruplex. To know the effect of the induced structure in a telomeric repeat by **1** binding on the telomere elongation, telomerase activity was evaluated by a modified telomeric repeat elongation (TRE) assay as previously described by Maesawa et al.[34] The TRE assay is a new method for direct measurement of telomerase activity using surface plasmon resonance (SPR). It is a non-PCR-based method and, therefore, is able to measure telomerase activity as the elongation rate without PCR-related artifacts and troublesome post-PCR procedures in various biological samples. In the TRE assay, telomere extracts (total cell extracts, 0.1 mg/mL) were injected onto the sensor surface where the biotinylated oligomer biotin−5′-d(TCC GTC GAG CAG AGT TAG GGT TAG GGT TAG GGT TAG GGT TAG GG)-3′ (**telo44**) (0.125 μg/mL) containing five telomeric repeats was immobilized. During the period of the injection, telomerase elongates **telo44** by incorporating dNTPs in the TRE buffer. The elongation of the oligomer immobilized on the SPR sensor resulted in an increase of the SPR signal reported in response units (RUs). The difference of SPR signals before the injection of telomere extracts and after regeneration of the sensor surface termed as the *e*-value was 115 RUs (Figure 10). In the presence of **1** (1 μM) in TRE buffer, the *e*-value was only 22 RUs, that is, one-fifth of that obtained by the injection of telomerase extracts without **1**. Injection of **1** without telomerase extracts produced an increasing SPR signal during the injection, showing a binding of **1** to the immobilized **telo44**, but resulted in no change of the SPR intensity after washing and conditioning. We have separately confirmed the binding of **1** to **telo9** in TRE buffer by UV spectral measurements. On the basis of these results, it is concluded that **1** inhibits the elongation of a telomeric repeat by the telomerase by the formation of a complex.

Conclusions

The data presented here constitute strong evidence for the formation of a complex between the naphthyridine dimer **1** and

(27) Ingham, K. C. *Anal. Biochem.* **1975**, *14*, 660−663.
(28) Beck, J. L.; Colgrave, M. L.; Ralph, S. F.; Sheil, M. M. *Mass Spectrom. Rev.* **2001**, *20*, 61−87.
(29) Sakamoto, S.; Fujita, M.; Kim, K.; Yamaguchi, K. *Tetrahedron* **2000**, *56*, 955−964.
(30) Kunimura, M.; Sakamoto, S.; Yamaguchi, K. *Org. Lett.* **2002**, *4*, 347−350.
(31) Yamanoi, Y.; Sakamoto, S.; Kusukawa, T.; Fujita, M.; Sakamoto, S.; Yamaguchi, K. *J. Am. Chem. Soc.* **2001**, *123*, 980−981.
(32) Sakamoto, S.; Yoshizawa, M.; Kusukawa, T.; Fujita, M.; Yamaguchi, K. *Org. Lett.* **2001**, *3*, 1601−1604.
(33) Sakamoto, S.; Imamoto, T.; Yamaguchi, K. *Org. Lett.* **2001**, *3*, 1793−1795.
(34) Maesawa, C.; Inaba, T.; Sato, H.; Iijima, S.; Ishida, K.; Terashima, M.; Sato, R.; Suzuki, M.; Yashima, A.; Ogasawara, S.; Oikawa, H.; Sato, N.; Saito, K.; Masuda, T. *Nucleic Acids Res.*, in press.

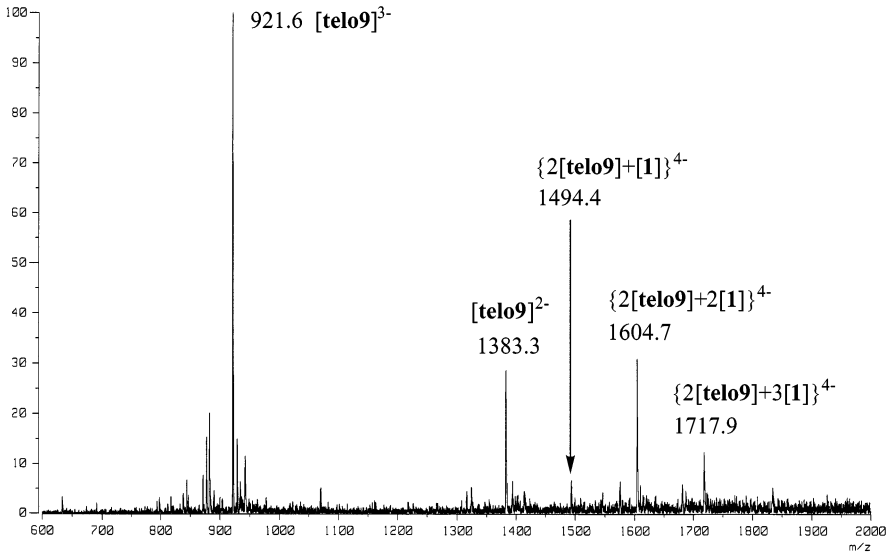

Figure 9. CSI-MS spectrum for the complex of **telo9** and **1**. The solution of **telo9** (18 μM) and **1** (85 μM) containing NH_4OAc (100 mM) in aqueous MeOH (40% v/v) was measured by CSI-MS. The sample solution was cooled at 7 °C during the injection with a flow rate of 0.5 mL/h.

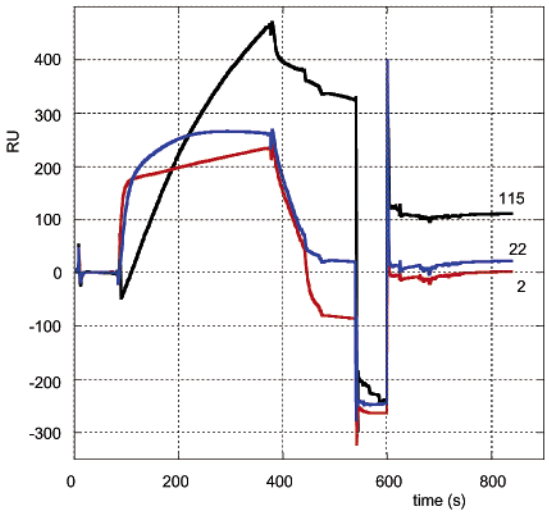

Figure 10. Sensorgrams obtained in the TRE assay for the inhibitory effects of **1** on telomeric repeat elongation. *e*-values of 115, 22, and 2 RUs were obtained for the injection of telomerase extracts (0.1 mg/mL) (black), telomerase extracts with **1** (1 μM) (blue), and only **1** (red), respectively.

the human telomeric sequence. Whereas the formation of a dimer duplex of **telo9**, d(TTAGGGTTA)/d(TTAGGGTTA), containing three G-G and two T-T mismatches is energetically unfeasible, strong stabilization of the G-G mismatch by **1** promotes the assembly of the sequence into a complex with **1**. TRE assay clearly showed that the complex induced by **1** binding inhibits the elongation of the telomeric repeat by telomerase.

Experimental Section

Measurements of CD Spectra. 1 (30 μM) was dissolved in a sodium cacodylate buffer (10 mM, pH 7.0) containing NaCl (100 mM) and **telo9** (5 μM). The CD spectrum of the solution was recorded on a JASCO J-805 spectrophotometer equipped with a temperature controller using a 1 cm path length cell at 25 °C.

Thermal Denaturation Profiles. 1 (30 μM) was dissolved in a sodium cacodylate buffer (10 mM, pH 7.0) containing **telo9** (5 μM, strand concentration) and NaCl (100 mM) at room temperature. The thermal denaturation profile of the sample was analyzed without any annealing on a SHIMADZU UV-2550 UV−vis spectrometer equipped with a Peltier temperature controller. The absorbance of the sample was monitored at 260 nm from 0 to 100 °C with a heating rate of 1 °C/min. The T_m value was determined by an average method.

Measurements of UV Absorption Spectra. 1 (20 μM) was dissolved in a sodium cacodylate buffer (10 mM, pH 7.0) containing NaCl (100 mM) and various concentrations of **telo9** (0−35 μM, final strand concentration). The UV absorption spectrum was recorded on a SHIMADZU UV-2550 spectrophotometer equipped with a Peltier temperature controller using a 1 cm path length cell at 20 °C.

Telomeric Repeat Elongation Assay. TRE assay was performed on a Biacore apparatus with the streptavidin-coated sensor chip (SA chip). 5′-Biotinylated oligomer biotin−5′-d(TCC GTC GAG CAG AGT-TAG GGT TAG GGT TAG GGT TAG GGT TAG GG)-3′ (**telo44**) (0.125 μg/mL) containing five telomeric repeats in 75 μL of HEPES buffer (10 mM HEPES, 150 mM NaCl, 10 mM $MgCl_2$, pH 7.4) was injected onto the SA chip at a flow rate of 5 μL/min at 37 °C. After 1500 RUs of oligomers had been immobilized, the chip surface was washed three times with 100 μL of 1% SDS in 10 mM HEPES to remove excess oligomers. Telomerase extracts (0.1 μg/mL) diluted in TRE buffer (10 mM HEPES, 150 mM NaCl, 10 mM $MgCl_2$, 2.5 mM dNTP, 10 mM EGTA, pH 7.4) were then injected across the sensor surface at a flow rate of 5 μL/min for 5 min in the absence and presence of **1** (1 μM). Subsequently, regeneration of the sensor surface was performed by washing with 1% SDS in 10 mM HEPES (100 μL) at a flow rate of 100 μL/min to remove all bound proteins. The baseline level was measured after the surface was conditioned with HEPES buffer for 3 min. SPR signals were expressed in response units (1 RU = 1 pg/mm^2), and real-time results were represented as a sensorgram. The amount of oligomer elongation was defined as the *e*-value (RUs), that is, the difference between the baseline level before injection of telomerase extracts and after the conditioning phase. The increased value (RUs) following immobilization was used to determine the number of moles of DNA at the chip surface, using an empirical relationship in which 1500 RUs was equivalent to 1.8 ng of DNA (1.276×10^{-13} mol of **telo44**). An extension of one base on all of the **telo44** would thus result in an increase of approximately 33.8 RUs. The rate of telomeric repeat elongation was calculated using the *e*-value.

Acknowledgment. This work was supported by a Grant-in-Aid for Scientific Research on Priority Areas (C) “Cancer” from the Ministry of Education, Culture, Sports, Science and Technology of Japan.

JA027055G